HYPERSPECTRAL CLASSIFICATION OF DISEASED TANGERINES

*

1st Pratyaksh Mundra
School of Computer
Science and Engineering
Vellore Institute of Technology
Chennai, India
pratyaksh.mundra28@gmail.com

2nd Gaurav Jayant Shrivastaa
School of Computer
Science and Engineering
Vellore Institute of Technology
Chennai, India
gauravjshrivastava10@gmail.com

3rd Dr. Sathian D
School of Computer
Science and Engineering
Vellore Intitute of Technology
Chennai, India
sathian.d@vit.ac.in

***Abstract*—This paper presents a comprehensive study on the classification of citrus fruits into anthracnose diseased (unhealthy) and non-diseased (healthy) categories using hyperspectral imaging. The dataset comprises hyperspectral images of citrus fruits, which were first subjected to Principal Component Analysis (PCA) for dimensionality reduction. Subsequently, various machine learning algorithms, including Support Vector Machine (SVM), Random Forest, and Logistic Regression, were applied. Additionally, deep learning models such as Inception-v3, VGG-16, and Double Branch Dual Attention models were employed to enhance classification performance. The experimental results demonstrate the effectiveness of both machine learning and deep learning approaches in accurately identifying diseased fruits, with deep learning models showing superior performance. This work highlights the potential of hyperspectral imaging combined with advanced classification techniques to improve disease detection in agricultural produce.**

***Index Terms*—Citrus Fruits, Antracnose, Hyper-spectral Images, Principal Component Analysis, Machine Learning Algorithms, Deep Learning Algorithms**

I. Introduction

Hyperspectral imaging (HSI) is a technology that has gained significant traction in the field of plant pathology because of its remarkable capabilities in disease detection. By capturing a broad spectrum of light, including wavelengths beyond the visible range, HSI offers a detailed view of the physical and chemical characteristics of plant tissues as different tissues and organisms radiate and absorb different types of spectrums. This detailed spectral information enables researchers to identify subtle changes associated with disease development, providing an invaluable tool for early detection and intervention.

In agricultural settings, where crop health is paramount, the early identification of diseases is crucial for mitigating potential losses and ensuring optimal yields. HSI's ability to detect anomalies in plant tissues before visible symptoms manifest empowers farmers and agronomists to implement timely and targeted disease management strategies. By intervening in the early stages of infection, growers can effectively contain the spread of diseases and minimize the impact on crop productivity.

In 2023/2024 the global production of oranges and tangerines was 48.8 and 38.0 metric tons [1] respectively. Around 50% of citrus crop around the world is wasted every year due to diseases and some common diseases found in citrus plants are anthracnose, citrus canker, melanose, and bacterial brown spot [2].

HSI facilitates non-destructive disease assessment, eliminating the need for invasive sampling procedures that could potentially harm plants or disrupt ongoing research efforts. This non-invasive approach not only streamlines disease monitoring but also allows for continuous observation of plant health over time. As a result, HSI has emerged as a valuable tool in the arsenal of plant pathologists, offering a reliable and efficient means of safeguarding crops against the threat of diseases [3].

Citrus anthracnose on tangerines [4], the primary subject of this study caused by the fungus Colletotrichum, is a significant disease affecting citrus crops. Hyperspectral imaging (HSI) has been employed to detect and manage this disease effectively. HSI captures a wide range of wavelengths across the electromagnetic spectrum, which allows for the identification of disease-specific spectral signatures in the infected plant tissues.

Recent studies have demonstrated the efficacy of HSI in identifying anthracnose in citrus plants with high accuracy. For instance, remote sensing techniques, including HSI, have been used to detect anthracnose diseases in tea plants, which share similarities with citrus plants in terms of foliar disease detection. These techniques achieved a detection accuracy of 98% at the leaf level and 94% at the pixel level, identifying disease-sensitive bands that are crucial for early detection .

Moreover, HSI combined with machine learning algorithms can classify the severity of the disease, which is essential for managing the spread and treatment of anthracnose in citrus crops [5]. The ability of HSI to detect the disease even before visible symptoms appear makes it a valuable tool for maintaining the health and quality of citrus fruits.

Compared to traditional disease detection methods in plants,

such as visual inspection and symptom-based diagnosis, rely on human assessments and may lead to delayed or inaccurate detection. Laboratory tests can confirm diseases but they are time-consuming. These methods lack efficiency and may result in misdiagnosis, leading to crop loss, making HSI detection a better option.

Our contributions are, firstly using a completely new dataset for analysis and training which will allow others to improve and validate the performance of existing models and Secondly doing a comparative analysis of various classic machine learning and deep learning models which will help determine which models to use in such applications. To achieve this objective, we are using hyperspectral images of tangerines via a visible and near-infrared (Vis-NIR) spectroscopy system. Subsequently, the hyperspectral data underwent preprocessing. In pursuit of comparative analysis, we employed classic ML techniques including Support Vector Machine (SVM), Random Forest, Naive Bayes, and Logistic Regression, alongside deep learning techniques comprising Inception V3 and VGG16.

II. Related Work

The topic of HSI has been extensively discussed by numerous researchers; therefore, various approaches exist in the literature. This section highlights related work in this area: The literature review encompasses a diverse array of studies focused on the application of hyperspectral imaging (HSI) across various domains, including agriculture, food quality analysis, plant disease detection, and remote sensing.

The primary objective of classification is to find related patterns across the dataset and make meaningful connections based on the labelled data and provide us with which category a particular image belongs to, Wang et al. (2021) [6] shows the uses of deep learning and classic machine learning based classification techniques for different classification tasks. Menesatti (2010) [7] shows how HSI can be used to not only classify the presence of diseases but we can also use it to track the progression of a disease making it a good option to detect a disease early as, when the disease progresses the reflectance of various wavelengths of a spectrum changes.

Blasco et al. (2007) [8] made a hyperspectral inspection setup which was used for sorting and identifying citrus fruits based on various flaws. They used data from near infrared, visible, UV and florescence spectra and received higher success rates when using non visible wavelengths then using only visible ones. Further work by Blasco et al. (2009) [9] using morphological defect features for this sorting increased the accuracy to 86% compared to just using RGB wavelengths alone.

Beyond just the fact that HSI allows us to identify diseases before they become visible therefore allowing for early detection but in a prior review, Gowen et al. (2007) [10] stated that the decrease in the cost of hyperspectral systems, commonly used in remote sensing can be used in labs for assessing food quality marking the emergence of HSI tools and techniques in food control and safety.

Lorente et al. (2012) [11] gave us a detailed survey of ways we can use various statistical techniques and methods to analyse hyperspectral images and He et al. (2018) [12] talks about new advances in spatial HSI and best practices which can we adopted for near infrared HSI as well.

HSI has been used in disease detection in 2 ways which are disease detection using spatial imaging and other is using near infrared imaging.

A. Near Infrared Imaging

Various methods from deep learning to machine learning can be used for disease detection Chu et al. (2018) [13] detected Aspergillus parasiticus and Aspergillus flavus growing on roses with an accuracy of 92.59% and 100% respectively using Support Vector Machine(SVM) and Principle Component Analysis(PCA). Nguyen et al [14]. (2021) studied the viral disease spread among grape vines through 2 months which was done with pixel wise classification(using SVM and Random forest) and 2d, and 3d CNN granting an accuracy of up to 96.75% for pixel-wise classification and 71% and 75% for 2d and 3d CNN respectively. Gao et al. (2019) [8] Used 3d CNN to prevent charcoal rot in plant stems captured using HSI. Lu et al. (2018) worked on identifying yellow leaf curl disease in tomato leaves getting an accuracy of up to a 100 percent. Zhang et al. (2018)[15] also used HSI to differentiate between different types of coffee.

Thomas et al. (2017) [16] provides a very detailed survey on disease detection using HSI on various plants it also describes various techniques for detections, environment for data collection and various preprocessing techniques.

B. Spatial Imaging

Spatial imaging involves taking images of terrain from very high and analysing them based on the spectrum they reflect.

Yang et al. (2018) [17] did a detailed review on Pavia university dataset where they got an accuracy of 98.2% and 97.21% for 3d-SVM and 3d-CNN respectively. Kumar et al. (2020) [18] also did a very detailed analysis of various feature extraction and classification techniques on Pavia and Salinas dataset showing promising results. Hong et al. (2022) [19] proposed a novel backbone network called SpectralFormer that uses transformers to learn spectral local sequence information from hyperspectral images and improve classification performance. It applies pixel-wise and patch-wise inputs and is validated on three hyperspectral datasets with good results.

Imani & Ghassemian (2020) [20] and Rasti et al. (2018) [21] provide various methods to improve the performance of our setup varying from noise reduction to feature fusion.

While spatial HSI is not withing the scope of this studies techniques can still be adapted from these studies to make our setup better.

III. Materials and Data Acquisition

A. Sample Preparation and Data Collection

The study uses South African mandarins of the Nadorcott variety, with 40 sound fruits of similar maturity and size

selected. These fruits underwent a cleaning process involving washing with a 2% sodium hypochlorite solution, followed by rinsing with tap water, air-drying, and storage under controlled conditions of 6^oC and 80% relative humidity. The anthracnose fungus used, C. gloeosporioides, was sourced from the Institute of Biotechnology, Zhejiang University. This fungus, isolated from naturally infected citrus anthracnose fruit, was cultured on a potato dextrose agar (PDA) medium. A suspension was then prepared with a concentration of approximately 1×10^6 CFU/ml using a haemocytometer plate for subsequent fungal inoculation experiments.

B. Hyperspectral Imaging System

The HSI system used for capturing citrus spectral data was the GaiaField-V10E from Jiangsu Dualix Spectral Imaging Technology Co., Ltd, based in Wuxi, Jiangsu, China. It comprised a hyperspectral camera and a data acquisition box. The camera model employed was the GaiaFieldPro-V10E, featuring a spectral range spanning 388–1025 nm, a spatial resolution of 960 × 1040 pixels, and 360 spectral channels. The data acquisition box housed four 50 W halogen lamps with a spectral range from 350 to 2500 nm, along with an adjustable loading platform. During acquisition, the citrus surface was positioned approximately 68 cm from the camera lens, with optimal imaging parameters determined by adjusting exposure time and focal length. These parameters included a motor forward speed of 0.46 mm/s and an exposure time of 10.8 ms.

C. Hyperspectral Image Acquisition

Hyperspectral images were obtained using a specialized camera capable of capturing 256 spectral bands, covering a spectral range from 386.70nm to 1016.70nm. Imaging took place in a controlled environment to maintain consistent lighting conditions and reduce external influences on spectral data as shown in figure 1. To ensure total coverage, each tangerine sample underwent imaging multiple times, with different orientations. This approach aimed to capture the complete range of spectral signatures present across the fruit's surface.

D. Data Organisation

The dataset structure was arranged to facilitate analysis and machine learning tasks, it has hyperspectral images alongside their respective health status labels. Each image possessed an initial shape of (696, 696, 256), of spectral information with a count of 179 the distribution is shown in Figure 3. During the data acquisition process, multiple images of each tangerine sample were captured from different angles to account for potential variations arising from fruit orientation.

E. Data Augmentation

The samples were physically augmented as seen in Figure 3 to introduce variety in the dataset and give the dataset the ability to detect disease in any way shape or form. Later the images were augmented again after preprocessing using digital

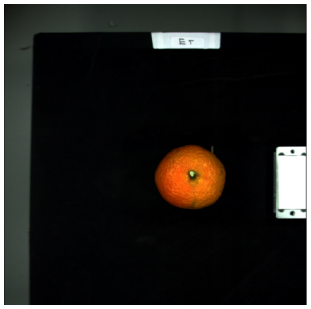

Fig. 1. Healthy Tangerine

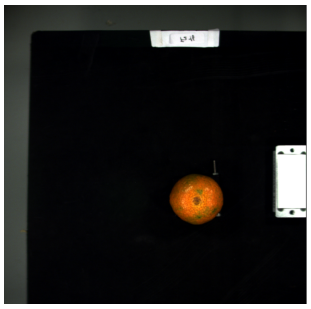

Fig. 2. Unhealthy Tangerine

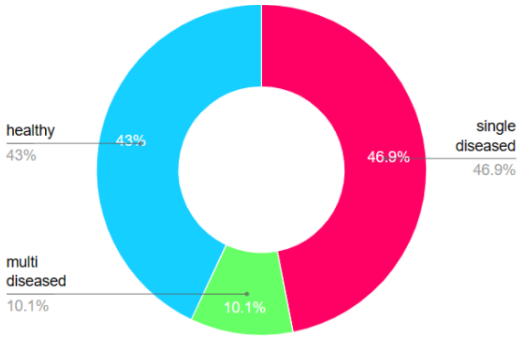

Fig. 3. The distribution of the labelled dataset

means so that the variety of the dataset increased and we could capture images with different formats, shapes and cameras and still be able to perform.

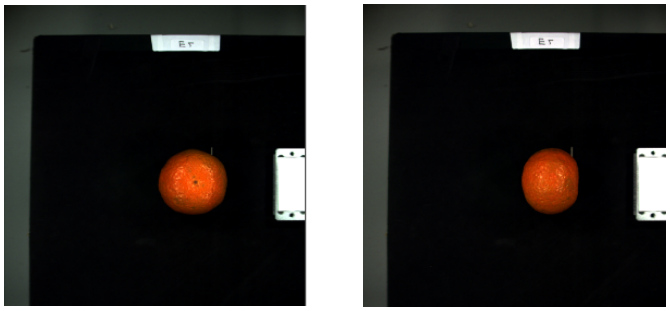

Fig. 4. Manual Augmentation

F. Prepossessing

Each datacube underwent manual cropping, isolating the orange's region of interest as shown in Figure 4. This targeted approach significantly reduced datacube size by an order of ten, enhancing focus on relevant features for more efficient model training.

Post-cropping, datacubes were uniformly padded and reshaped to a consistent size of (160,160). This standardization ensured consistency across the dataset, facilitating streamlined processing and analysis.

Principal Component Analysis (PCA) [22] is a statistical technique used to reduce the dimensionality of high-

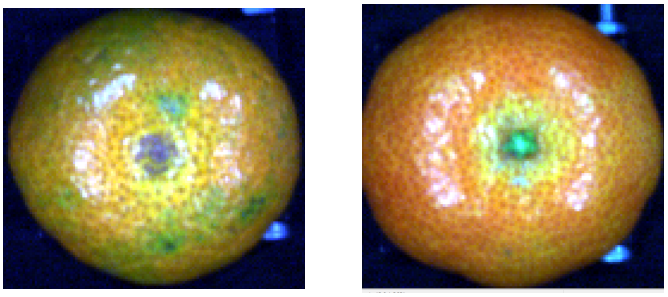

Fig. 5. Hyperspectral image in RGB colour after cropping to ROI. (a) Unhealthy Tangerine. (b) Healthy Tangerine

dimensional data while preserving most of its variance. It identifies the directions (or principal components) along which the data varies the most and projects the data onto these components. In doing so, PCA transforms the original features into a new set of linearly uncorrelated variables called principal components. As seen in Figure 5 it was used to reduce the spectral channels to three, reducing computational complexity while keeping important information. Furthermore, digital augmentation techniques such as flips, zooms, and rotations were systematically applied, improving the dataset with diverse variations to enhance the robustness and generalization of the model.

After PCA the images generated were digitally augmented by performing random flips, zooms and rotations as seen in Figure 6 to introduce more variety and generalization.

Post-cropping, datacubes were uniformly padded and reshaped to a consistent size of (160,160). This standardization ensured consistency across the dataset, facilitating streamlined processing and analysis.

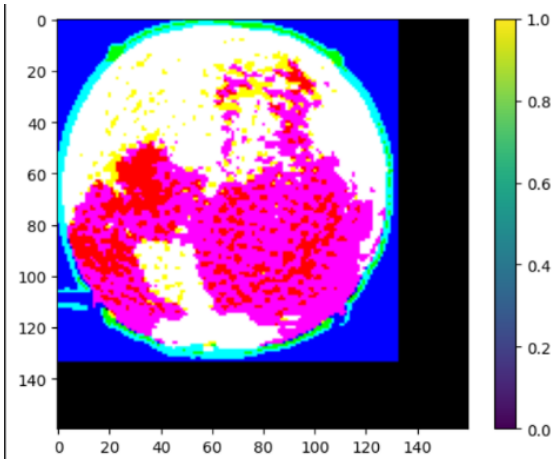

Fig. 6. Sample image after PCA and Padding

IV. Methodology

For the classification of diseased and not-diseased tangerines, we went ahead with a focus on classical ml techniques as they are not only fast but they also need less data. We also used transfer learning architecture primarily trained on ImageNet as they are specialized in image classification.

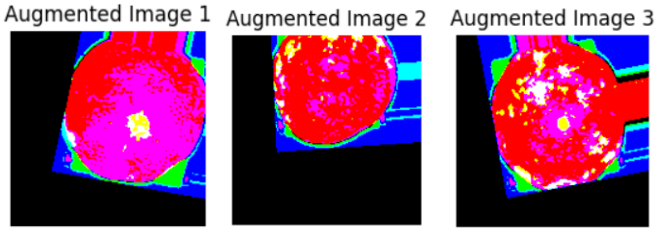

Fig. 7. Digitally Augmented Images

A. Use of Classical ML Models

1) Support Vector Machines(SVM): SVMs are powerful machine-learning algorithms used for both classification and regression tasks. The key idea behind SVMs is to find an optimal hyperplane in an N-dimensional space that maximally separates data points belonging to different classes. This hyperplane ensures that the margin between the closest points of different classes is as wide as possible [23]. SVMs are versatile and efficient, handling high-dimensional data and nonlinear relationships. In the context of HSI classification, SVM analyses the spectral signatures of pixels and works to identify the hyperplane that best separates these signatures into meaningful classes, facilitating accurate categorization of materials or features within the hyperspectral scene. This capability is particularly advantageous in HSI applications where subtle spectral differences hold crucial information regarding the composition or characteristics of the imaged objects [24].

2) Random Forest: Random Forest (RF) is a classification method that combines lots of tree-like classifiers. Following the training of these classifiers, RF uses a voting mechanism to find the class for a particular value class [25]. Random Forest (RF) demonstrates high accuracy and efficiency in data processing. The final classification is determined by the majority vote across all trees, ensuring great predictions. Additionally, a subset of the training data is set aside for evaluating the accuracy of the model, enhancing its reliability [26].

It effectively captures complex interactions between features, making it well-suited for HSI classification tasks where the data is high-dimensional. Random Forest performs well even without extensive hyperparameter tuning and is less prone to overfitting compared to individual decision trees, making it a preferred choice for HSI classification.

3) Naive Bayes: Naive Bayes classifiers, rooted in Bayes' Theorem, are renowned for their simplicity and efficiency in machine learning, despite their "naive" assumption of feature independence. These classifiers predict the probability of an instance belonging to a class based on a given set of feature values, if each feature contributes independently to the prediction. Despite this simplification, Naive Bayes classifiers perform remarkably well in various applications,

using probabilistic classification to calculate the likelihood of an input belonging to a particular class [27].

Naive Bayes, while simple, is computationally efficient and performs surprisingly well, especially when the assumption of independence between features holds approximately true. This makes it suitable for quick analysis of HSI data and can be particularly useful in scenarios where resources are limited.

4) Logistic Regression: Logistic regression is a statistical method used for binary classification. It predicts the probability that a given data point belongs to a particular category. The core concept is of the logistic function, which is an S-shaped curve that can take any real-valued number and map it between 0 and 1, but never exactly at those limits. Logistic Regression, another simple yet powerful algorithm, is interpretable and suitable for binary classification tasks within HSI data. With appropriate regularization, it can handle multicollinearity in the data and allows for examining the impact of each spectral band on the classification outcome, providing valuable insights.

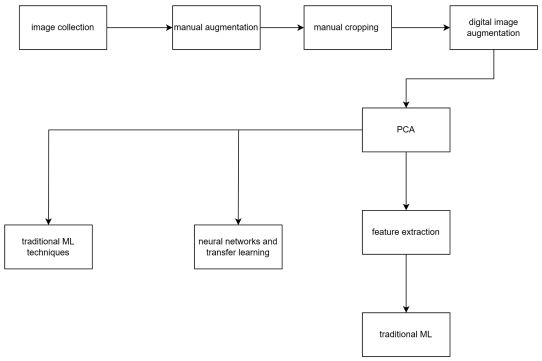

Fig. 8. Flow Diagram of Model Training

B. Use of DL Models

1) Inception V3: The Inception V3 [28] model is a convolutional neural network (CNN) that's part of the Inception family, known for its efficiency and accuracy in image classification tasks. It is the third version of the Inception models, originally introduced during the ImageNet Recognition Challenge. Since it is trained on ImageNet, it makes inception an ideal candidate for image classification tasks and takes very little fine-tuning on top of the base model for it to work with HSI images.

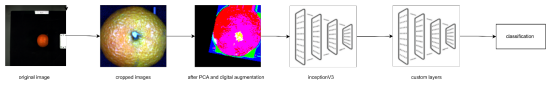

Fig. 9. Inception V3 Flow Diagram

2) VGG16: VGG16 is a deep convolutional neural network model that has become a benchmark for image classification due to its that have weights. The architecture features thirteen convolutional layers, five max-pooling layers, and three fully connected layers. The convolutional layers use small (3X3) filters, which allow the network to capture more complex features at each layer [29].

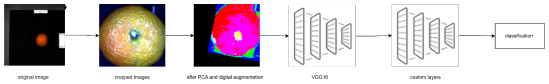

Fig. 10. VGG16 Flow Diagram

*3) CNN (**Proposed Model**):* Convolutional Neural Networks (CNNs) [30] are sophisticated deep learning models extensively used in visual imagery analysis. These networks consist of multiple layers, including input, hidden, and output layers, which often encompass convolutional, pooling, fully connected, and normalization layers. Convolutional layers employ filters that learn to detect various features such as edges and textures, which are then propagated through the network. Pooling layers reduce the spatial dimensions of the data, which helps prevent overfitting and lowers computational demands. The fully connected layers, placed near the end of the network, are responsible for complex decision-making tasks. CNNs are trained and optimized using techniques like backpropagation and gradient descent. Their utility extends beyond image classification to include applications in object detection, video analysis, and natural language processing, thanks to their capability to manage data in grid-like structures. CNNs' proficiency in hierarchical feature detection has fueled their widespread adoption across numerous fields.

CNNs are particularly adept at processing image data, including Hyperspectral Imaging (HSI), by automatically learning hierarchical features and capturing spatial dependencies that are crucial for deciphering complex patterns within the data. Architectures such as VGG, ResNet, and Inception have shown significant success in various image classification tasks, including HSI classification.

As depicted in Figure 7, the HSI-CNN model, that we propose to test, begins with a Conv2D input layer comprising 32 filters of size 3x3 with ReLU activation, specifically tailored for processing 160x160 RGB images. This layer serves as the foundation for feature extraction by applying filters across the input data.

Following this, a MaxPooling2D layer with a 2x2 pool size is utilized to reduce the spatial dimensions by half, enhancing computational efficiency and reducing the likelihood of overfitting. The model then progresses through two additional Conv2D layers, each incorporating 64 and 128 filters of size 3x3 with ReLU activation, which are structured to extract increasingly complex features.

Subsequent to these convolutional operations, a Flatten layer is employed to convert the resulting feature maps into a one-dimensional vector, preparing the data for the Dense layers. The model concludes with two Dense layers: the first with 512 neurons and ReLU activation, and the final layer with a single neuron and sigmoid activation, designed to produce a binary output that indicates the likelihood of the input image being classified as belonging to the positive class.

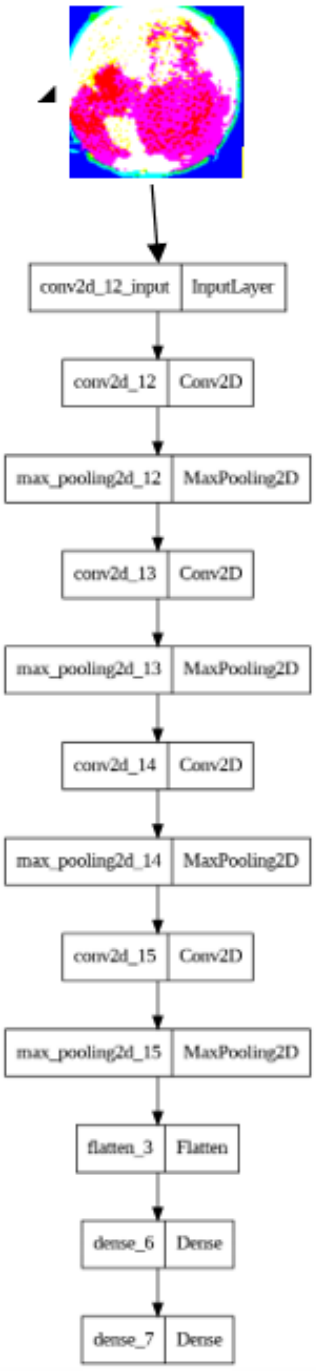

Fig. 11. Used CNN Architecture

4) Double Branch Dual Attention: The Double Branch Dual Attention (DBDA) [31] network is an advanced deep learning model designed to enhance the detection of infected regions in tangerines using hyperspectral image analysis. This network is particularly well-suited for agricultural applications where precise identification of diseased areas is crucial for timely intervention and crop management. The key features include:

1. Double Branch Architecture:

- The DBDA network consists of two parallel branches that process spectral and spatial information separately.
- *Spectral Branch*: This branch focuses on the spectral characteristics of the hyperspectral data, capturing subtle variations in the wavelengths that indicate the presence of disease.
- *Spatial Branch*: This branch analyzes the spatial context of the images, identifying patterns and structures that correspond to infected regions.

2. Dual Attention Mechanism:

- The network employs dual attention mechanisms to enhance the feature representation from both branches.
- *Spectral Attention*: This mechanism emphasizes the most relevant spectral bands that contribute to identifying diseased areas, effectively filtering out noise.
- *Spatial Attention*: This mechanism highlights critical spatial features, ensuring that the network focuses on regions with significant disease-related patterns.

3. Integration and Classification:

- After processing through the dual branches and attention mechanisms, the features are integrated to form a comprehensive representation of the hyperspectral image.
- The integrated features are then passed through fully connected layers for classification, distinguishing between healthy and infected regions.

In the context of tangerine disease detection, the DBDA network is trained on hyperspectral images that include both healthy and infected samples. The hyperspectral images provide detailed spectral information across numerous bands, capturing subtle differences that are indicative of disease. The DBDA network processes these images to accurately identify and localize infected regions, enabling precise and early intervention.

Overall, the DBDA network represents a significant advancement in hyperspectral image analysis, offering a powerful tool for agricultural disease detection and management. Its ability to integrate and focus on both spectral and spatial features makes it particularly effective for complex tasks such as detecting infected regions in tangerines.

C. Feature Extraction

Due to the prowess of InceptionV3 in image classification tasks and the ability of classical ML models to work well on less data, and the fact that they are faster led us to explore the use of inception 3 as a feature extractor and then using ml models that we previously used on it as seen in figure 6.

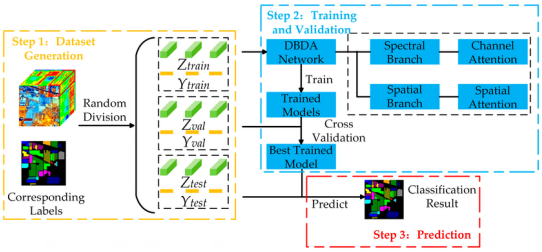

Fig. 12. DBDA Architecture

Incorporating Inception v3 as a feature extractor for traditional machine learning algorithms resulted in significant performance improvements across the board. Adaboost, SVM, Random Forest, Logistic Regression, and Naive Bayes all experienced notable increases in accuracy when using features extracted by Inception v3.

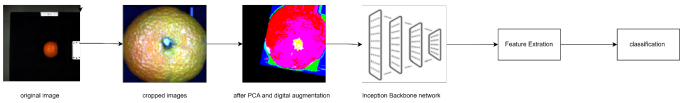

Fig. 13. Flow Diagram of Feature extraction method

V. Results

As seen in Table I, various models were evaluated for their performance.

Observing from Table I, we can see that in terms of the best overall traditional model, Adaboost with Decision Trees performed well, while Adaboost with Random Forest also exhibited similar accuracy. Although Adaboost with Random Forest had better recall and precision of 91% and 93%, respectively, making it a potentially superior model for detecting healthy and unhealthy tangerines.

Inception V3 had the best performance with an accuracy of 87% among all the deep learning and transfer learning models tested. Being trained on ImageNet, Inception V3 excels in image recognition tasks, making it a strong candidate. VGG16 also showed competitive performance with a precision of 94% and recall of 92%, though it had a slightly lower accuracy of 81%.

When it comes to feature extraction, we can use Inception V3 for that task and then train the model using Adaboost, achieving an accuracy of 95% with this approach. This takes advantage of the superior feature extraction capability of the Inception model and the advantage of traditional ML algorithms in training models with smaller datasets.

The CNN model demonstrated exceptional performance with an accuracy of 95%, a precision of 91%, a recall of 93%, and an F1-score of 94%, making it a strong contender for hyperspectral image classification tasks. However, the DBDA model, despite its high computational time of 80.6 seconds, showed respectable performance with an accuracy of 90%, precision of 87%, and recall of 89%.

The CNN2D model achieved an accuracy of 86%, precision of 79%, recall of 94%, and an F1-score of 86%. The training time for this model was relatively short, 42.106 seconds. The high recall of the model indicates its effectiveness in identifying diseased tangerines, which is crucial for early detection and prevention of crop loss. However, the precision value suggests a significant number of false positives, meaning that some healthy tangerines were incorrectly classified as diseased.

The use of PCA to reduce the hyperspectral image bands to three principal components likely contributed to the model's efficiency. PCA helps in dimensionality reduction by transforming the original data into a set of linearly uncorrelated variables (principal components) that capture the most variance in the data. This reduction in dimensionality not only speeds up the training process, but also helps mitigate the curse of dimensionality, a common challenge in hyperspectral image analysis.

However, the CNN3D model demonstrated an accuracy of 86%, precision of 100%, recall of 69%, and an F1-score of 89%. The training time for this model was significantly longer at 343.33 seconds. The perfect precision score indicates that the model was very accurate in identifying healthy tangerines, with no false positives. However, the recall value was comparatively low, suggesting that the model missed a substantial number of diseased tangerines.

The use of 81 bands of the hyperspectral image in the CNN3D model provided a richer set of features for classification. The 3D convolutional layers are capable of capturing spatial and spectral information simultaneously, which is beneficial for hyperspectral image analysis. Despite this advantage, the model's lower recall indicates that it struggled to generalize well to the diseased class, possibly due to the increased complexity and the need for more training data to fully exploit the additional bands.

Comparing the training times of these models, it is evident that the CNN2D model is significantly more efficient than the CNN3D model. The CNN2D model required only 42.106 seconds for training, while the CNN3D model took 343.33 seconds. This stark contrast highlights the computational expense associated with processing a higher number of spectral bands and the increased complexity of 3D convolutional layers. The DBDA model also had a relatively high training time of 80.6 seconds, reflecting the added complexity of dual attention mechanisms and the need for extensive computations.

Both models exhibited an accuracy of 86%, highlighting their effectiveness in classifying tangerines as either healthy or diseased. However, their performance metrics reveal different strengths and weaknesses. The CNN2D model's higher recall and shorter training time make it more suitable for scenarios where timely detection of diseased tangerines is critical. Its use of PCA to reduce the number of bands to three principal components ensures that the model remains computationally efficient while maintaining a high level of accuracy.

In contrast, the perfect precision of the CNN3D model indicates its reliability in identifying healthy tangerines, mak-

TABLE I
PERFORMANCE METRICS OF VARIOUS MODELS

Model	Accuracy	Precision	Recall	F1-Score	Training Time (Seconds)
SVM	0.81	0.89	0.85	0.86	5.42
Random Forest	0.86	0.92	0.89	0.90	0.06
Naïve Bayes	0.82	0.86	0.81	0.88	0.29
Logistic Regression	0.83	0.90	0.87	0.87	0.04
InceptionV3	0.87	0.96	0.94	0.90	0.29
VGG16	0.81	0.94	0.92	0.86	3.65
HSI CNN (Proposed)	0.95	0.91	0.93	0.94	3.2
CNN2D Simple	0.86	0.79	0.94	0.86	42.106
CNN3D Simple	0.86	1.00	0.69	0.89	343.33
DBDA	0.90	0.87	0.89	0.88	80.6
SVM with Inception	0.92	0.96	0.95	0.94	3.44
RF with Inception	0.91	0.90	0.86	0.94	0.01
LR with Inception	0.90	0.95	0.93	0.93	0.01
NB with Inception	0.80	0.90	0.87	0.85	0.08

ing it valuable in applications where false positives must be minimized. However, its lower recall and longer training time suggest that it might require further optimization and potentially more training data to improve its generalization to the diseased class.

The comparison between CNN2D and CNN3D models underscores the trade-offs between computational efficiency and model complexity in hyperspectral image analysis. While CNN2D models can be effective with dimensionality reduction techniques like PCA, CNN3D models have the potential to capture more detailed spatial and spectral features, albeit at the cost of increased computational requirements.

For practical applications, the choice between CNN2D and CNN3D models should be guided by the specific requirements of the task, including the need for precision, recall, and computational resources. Future research could explore hybrid approaches that combine the strengths of both models, such as using PCA for initial dimensionality reduction followed by 3D convolutional layers to further refine the feature extraction process.

In conclusion, both CNN2D and CNN3D models offer valuable insights for hyperspectral image classification. The CNN2D model, with its high recall and efficiency, is well suited for rapid detection of diseased tangerines, while the CNN3D model, with its high precision, is ideal for applications where minimizing false positives is crucial. By understanding the trade-offs and leveraging the strengths of each approach, we can develop more robust and accurate models for agricultural disease detection.

1) Proposed CNN Model: HSI-CNN: The performance metrics presented in Table I highlight the effectiveness of our proposed HSI-CNN model in comparison to other models. Our model achieves the highest accuracy (0.95), which indicates its strong ability to correctly classify both positive and negative samples. The precision (0.91) of the HSI-CNN is also notably high, demonstrating that the model is highly reliable when it predicts a positive class, with fewer false positives.

In terms of recall (0.93), the HSI-CNN excels at identifying true positives, indicating that it effectively detects the diseased Tangerine cases. The F1-Score (0.94) further corroborates the model's balanced performance between precision and recall, showing that it maintains a good trade-off between sensitivity and specificity.

Additionally, the training time for our HSI-CNN model is only 3.2 seconds, which is significantly lower compared to more complex models like CNN3D Simple and DBDA, which take 343.33 seconds and 80.6 seconds, respectively. This demonstrates that our model is not only highly accurate and reliable but also efficient in terms of computational resources and time, making it a practical choice for real-time applications.

Overall, our proposed HSI-CNN model outperforms the other models in the table across multiple metrics, solidifying its robustness and efficiency in handling the classification task for HSI of diseased Tangerine.

A. Importance of This Research

As already stated, the loss of crop due to diseases is of major concern, leading to low yields, financial losses, and potential human health issues. Agricultural crops are the backbone of food security and economic stability for many regions, and any threat to their productivity has far-reaching consequences. Management of disease in crops such as tangerines is critical not only to maintain high yields but also to ensure the quality and safety of the product. Traditional methods of disease detection often rely on manual inspection, which can be time-consuming, labor-intensive, and prone to human error. These limitations necessitate the development of advanced automated approaches that can reliably identify and classify diseased crops.

The focus of this research is to create and evaluate a methodology that uses recently developed hyperspectral imaging (HSI) tools and methodologies to identify and classify diseased tangerines from healthy ones. Hyperspectral imaging captures a wide range of spectral information across numerous bands, providing detailed information on the chemical and physical properties of crops. This level of detail is instrumental in detecting subtle changes in the crop's condition that are not visible to the naked eye.

The study aims to test the performance of this advanced methodology and its potential to improve the classification of HSI. By leveraging the rich spectral data obtained from hyperspectral images, the research seeks to enhance both the accuracy and computational efficiency of disease detection. High accuracy ensures that diseased crops are correctly identified, reducing the risk of spread and allowing for timely intervention. Improved computational efficiency makes the technology feasible for real-time applications, enabling continuous monitoring and early detection.

The integration of machine learning algorithms, particularly Convolutional Neural Networks (CNNs) and advanced models like the Double Branch Dual Attention (DBDA) network, plays a pivotal role in this research. These algorithms can learn complex patterns and features from the hyperspectral data, significantly outperforming traditional image processing techniques. The CNN2D and CNN3D models, for instance, demonstrate the capability of deep learning models to handle different dimensions of spectral data, providing valuable comparisons and insights into their respective strengths and weaknesses.

Moreover, the use of transfer learning models such as InceptionV3 further enhances the robustness of the classification system. By transferring knowledge from pre-trained models on large datasets like ImageNet, the research leverages established feature extraction capabilities, reducing the need for extensive training on smaller, specific datasets. This approach not only speeds up the training process but also improves the generalization of the model, making it more adaptable to varying conditions and types of diseases.

The significance of this research extends beyond just tangerines. The methodologies and findings can be applied to a wide range of crops, contributing to the broader field of precision agriculture. Precision agriculture involves the use of technology to optimize field-level management in crop farming. The ability to accurately and efficiently detect diseases at an early stage can lead to better resource management, reduced use of pesticides, and ultimately, more sustainable farming practices.

In addition, the successful implementation of these techniques can have economic benefits for farmers by reducing losses and increasing productivity. It can also enhance food safety and quality for consumers by ensuring that only healthy produce reaches the market. The insights gained from this research can inform policymakers and agricultural stakeholders about the best practices for integrating advanced imaging and machine learning technologies into existing agricultural frameworks.

In conclusion, this research addresses a critical need in the agricultural sector by providing a sophisticated, accurate, and efficient method for disease detection in crops. By harnessing the power of hyperspectral imaging and advanced machine learning algorithms, this study lays the groundwork for future innovations in crop disease management, with the potential to significantly impact food security and agricultural sustainability.

B. Limitations and Future Work

Limitations in this study include reliance on a single dataset, potentially biasing results, and limiting generalizability. Dataset size and diversity constraints impact the robustness of the model. Ideally, the models should be tested on multiple datasets to demonstrate their generalizability and robustness. However, due to limitations in time and resources, this was not possible.

Furthermore, while the Inception V3 model combined with Adaboost shows promising results, further improvements could be achieved by exploring other transfer learning models such as ResNet or DenseNet which might offer better feature extraction capabilities.

Future studies could address the limitations of this research by incorporating multiple datasets, which can help avoid infeasibility during real-time tests. Additionally, optimizing the DBDA model to reduce computational time while maintaining or improving accuracy could be a significant area of future research. Finally, exploring the integration of more sophisticated data augmentation techniques and the use of advanced ensemble methods could further enhance the model's performance.

This research shows promising results, but highlights the need for continued exploration and development in the field of hyperspectral image analysis for agricultural applications. By addressing the mentioned limitations, future research can build on these findings to create more robust and reliable models for disease detection in tangerines and other crops.

REFERENCES

[1] Reed Blauer, "United States Department of Agriculture Foreign Agricultural Service Record Exports Forecast for Egypt Oranges," 2024. [Online]. Available: https://public.govdelivery.com/accounts/USDAFAS/subscriber/new

[2] Institute of Electrical and Electronics Engineers Bombay Section, Annual IEEE Computer Conference, International Conference for Convergence of Technology 2014.04.06-08 Pune, and I2CT 2014.04.06-08 Pune, 2014 International Conference for Convergence of Technology (I2CT) 6-8 April 2014, Pune.

[3] L. W. Kuswidiyanto, H. H. Noh, and X. Han, "Plant Disease Diagnosis Using Deep Learning Based on Aerial Hyperspectral Images: A Review," Remote Sensing, vol. 14, no. 23. MDPI, Dec. 01, 2022. doi: 10.3390/rs14236031.

[4] S. Phoulivong, "Cross infection of Colletotrichum species; a case study with tropical fruits," Current Research in Environmental & Applied Mycology, vol. 2, no. 2, pp. 99–111, 2012, doi: 10.5943/cream/2/2/2.

[5] A. K. Saini, R. Bhatnagar, and D. K. Srivastava, "Automatic Detection and Recognition of Citrus Fruit & Leaves Diseases for Precision Agriculture," Journal of Universal Computer Science, vol. 28, no. 9, pp. 930–948, 2022, doi: 10.3897/jucs.94133.

[6] P. Wang, E. Fan, and P. Wang, "Comparative analysis of image classification algorithms based on traditional machine learning and deep learning," Pattern Recognit Lett, vol. 141, pp. 61–67, Jan. 2021, doi: 10.1016/J.PATREC.2020.07.042.

[7] P. Menesatti, C. Costa, and J. Aguzzi, "Quality Evaluation of Fish by Hyperspectral Imaging," in Hyperspectral Imaging for Food Quality Analysis and Control, Elsevier, 2010, pp. 273–294. doi: 10.1016/B978-0-12-374753-2.10008-5.

[8] J. Blasco, N. Aleixos, J. Gómez, and E. Moltó, "Citrus sorting by identification of the most common defects using multispectral computer vision," J Food Eng, vol. 83, no. 3, pp. 384–393, Dec. 2007, doi: 10.1016/J.JFOODENG.2007.03.027.

[9] J. Blasco, N. Aleixos, J. Gómez-Sanchís, and E. Moltó, "Recognition and classification of external skin damage in citrus fruits using multispectral data and morphological features," Biosyst Eng, vol. 103, no. 2, pp. 137–145, Jun. 2009, doi: 10.1016/J.BIOSYSTEMSENG.2009.03.009.

[10] A. A. Gowen, C. P. O'Donnell, P. J. Cullen, G. Downey, and J. M. Frias, "Hyperspectral imaging – an emerging process analytical tool for food quality and safety control," Trends Food Sci Technol, vol. 18, no. 12, pp. 590–598, Dec. 2007, doi: 10.1016/J.TIFS.2007.06.001.

[11] D. Lorente, N. Aleixos, J. Gómez-Sanchis, S. Cubero, O. L. García-Navarrete, and J. Blasco, "Recent Advances and Applications of Hyperspectral Imaging for Fruit and Vegetable Quality Assessment," Food and Bioprocess Technology, vol. 5, no. 4. pp. 1121–1142, May 2012. doi: 10.1007/s11947-011-0725-1.

[12] L. He, J. Li, C. Liu, and S. Li, "Recent Advances on Spectral-Spatial Hyperspectral Image Classification: An Overview and New Guidelines," IEEE Transactions on Geoscience and Remote Sensing, vol. 56, no. 3, pp. 1579–1597, Mar. 2018, doi: 10.1109/TGRS.2017.2765364.

[13] X. Chu et al., "Growth identification of Aspergillus flavus and Aspergillus parasiticus by visible/near-infrared hyperspectral imaging," Applied Sciences (Switzerland), vol. 8, no. 4, Mar. 2018, doi: 10.3390/app8040513.

[14] C. Nguyen, V. Sagan, M. Maimaitiyiming, M. Maimaitijiang, S. Bhadra, and M. T. Kwasniewski, "Early detection of plant viral disease using hyperspectral imaging and deep learning," Sensors (Switzerland), vol. 21, no. 3, pp. 1–23, Feb. 2021, doi: 10.3390/s21030742.

[15] C. Zhang, F. Liu, and Y. He, "Identification of coffee bean varieties using hyperspectral imaging: Influence of preprocessing methods and pixel-wise spectra analysis," Sci Rep, vol. 8, no. 1, Dec. 2018, doi: 10.1038/s41598-018-20270-y.

[16] S. Thomas et al., "Benefits of hyperspectral imaging for plant disease detection and plant protection: a technical perspective," Journal of Plant Diseases and Protection, vol. 125, no. 1. Springer Berlin Heidelberg, pp. 5–20, Feb. 01, 2018. doi: 10.1007/s41348-017-0124-6.

[17] X. Yang, Y. Ye, X. Li, R. Y. K. Lau, X. Zhang, and X. Huang, "Hyperspectral image classification with deep learning models," IEEE Transactions on Geoscience and Remote Sensing, vol. 56, no. 9, pp. 5408–5423, Sep. 2018, doi: 10.1109/TGRS.2018.2815613.

[18] B. Kumar, O. Dikshit, A. Gupta, and M. K. Singh, "Feature extraction for hyperspectral image classification: a review," International Journal of Remote Sensing, vol. 41, no. 16. Taylor and Francis Ltd., pp. 6248–6287, Aug. 17, 2020. doi: 10.1080/01431161.2020.1736732.

[19] D. Hong et al., "SpectralFormer: Rethinking Hyperspectral Image Classification with Transformers," Jul. 2021, doi: 10.1109/TGRS.2021.3130716.

[20] M. Imani and H. Ghassemian, "An overview on spectral and spatial information fusion for hyperspectral image classification: Current trends and challenges," Information Fusion, vol. 59, pp. 59–83, Jul. 2020, doi: 10.1016/j.inffus.2020.01.007.

[21] B. Rasti, P. Scheunders, P. Ghamisi, G. Licciardi, and J. Chanussot, "Noise reduction in hyperspectral imagery: Overview and application," Remote Sens (Basel), vol. 10, no. 3, Mar. 2018, doi: 10.3390/rs10030482.

[22] J. Lever, M. Krzywinski, and N. Altman, "Points of Significance: Principal component analysis," Nature Methods, vol. 14, no. 7. Nature Publishing Group, pp. 641–642, Jun. 29, 2017. doi: 10.1038/nmeth.4346.

[23] D. A. Pisner and D. M. Schnyer, "Support vector machine," in Machine Learning: Methods and Applications to Brain Disorders, Elsevier, 2019, pp. 101–121. doi: 10.1016/B978-0-12-815739-8.00006-7.

[24] D. K. Pathak, S. K. Kalita, and D. K. Bhattacharya, "Hyperspectral image classification using support vector machine: a spectral spatial feature based approach," Evol Intell, vol. 15, no. 3, pp. 1809–1823, Sep. 2022, doi: 10.1007/s12065-021-00591-0.

[25] A. K. Bhatt, D. Pant, and R. Singh, "An analysis of the performance of Artificial Neural Network technique for apple classification," AI Soc, vol. 29, no. 1, pp. 103–111, Feb. 2014, doi: 10.1007/s00146-012-0425-z.

[26] P. Quesada-Barriuso, F. Arguello, and D. B. Heras, "Spectral-spatial classification of hyperspectral images using wavelets and extended morphological profiles," IEEE J Sel Top Appl Earth Obs Remote Sens, vol. 7, no. 4, pp. 1177–1185, 2014, doi: 10.1109/JSTARS.2014.2308425.

[27] C. Sammut and G. I. Webb, "N Naïve Bayes Motivation and Background," 2010. doi: https://doi.org/10.1007/978-0-387-30164-8-576.

[28] C. Szegedy et al., "Going Deeper with Convolutions," Sep. 2014, [Online]. Available: http://arxiv.org/abs/1409.4842

[29] K. Simonyan and A. Zisserman, "Very Deep Convolutional Networks for Large-Scale Image Recognition," Sep. 2014, [Online]. Available: http://arxiv.org/abs/1409.1556

[30] K. O'Shea and R. Nash, "An Introduction to Convolutional Neural Networks," Nov. 2015, [Online]. Available: http://arxiv.org/abs/1511.08458

[31] Li, R., Zheng, S., Duan, C., Yang, Y., & Wang, X. (2020). Classification of hyperspectral image based on double-branch dual-attention mechanism network. Remote Sensing, 12(3), 582.